

1 *This is a non-peer-reviewed preprint submitted to EarthArXiv. The manuscript has been submitted*
2 *to the ISME Journal for publication, and it is currently under review. Please note that subsequent*
3 *versions of this manuscript may have slightly different content. If accepted, the final version of the*
4 *manuscript will be available via the 'Peer-reviewed Publication DOI' link on this webpage.*
5

6 7 **Microbial growth inhibition by compacted bentonite after an 8.5-year** 8 ***in-situ* incubation**

9
10 Natalia Jakus^{1#}, Nikitas Diomidis², Rizlan Bernier-Latmani¹

11 ¹Environmental Microbiology Laboratory, École Polytechnique Fédérale de Lausanne
12 (EPFL), Switzerland

13 ²National Cooperative for the Disposal of Radioactive Waste (NAGRA), Switzerland
14

15 **Contact addresses (in order):**

16 #Corresponding author: natalia.jakus@epfl.ch, @NataliaJakus@mastodon.social

17 nikitas.diomidis@nagra.ch

18 rizlan.bernier-latmani@epfl.ch
19
20

21 **Abstract**

22 Compacted bentonite in future deep geological repositories for the disposal of nuclear
23 waste will create an extreme, energy-limited environment for microorganisms, yet the
24 long-term implications for microbial community structure and the potential emergence
25 of sulfate-reducing bacteria (SRB) remain uncertain. Here, we use an 8.5-year *in-situ*
26 incubation experiment in an anoxic Opalinus Clay borehole, integrating observations
27 from successive retrieval phases after 1.5, 5.5, and 8.5 years, to examine changes in
28 microbial persistence in compacted Wyoming bentonite across three dry densities
29 (1.25, 1.45, and 1.55 g/cm³). 16S rRNA gene quantification and sequencing showed
30 that microbial cell numbers remained low and declined significantly over time at all
31 densities, with density as the primary driver and time as the dominant secondary driver
32 of community change. After 8.5 years, SRB were detected only in the rare biosphere
33 (<0.1% relative abundance), although they were recoverable by cultivation, indicating
34 survival rather than growth. Altogether, these results support limited concern about the

35 progressive enrichment of corrosion-inducing microorganisms following oxygen
36 depletion and demonstrate that bentonite compaction at 1.25 g/cm³ is sufficient to
37 inhibit microbial growth, providing an effective biological barrier.

38

39 **Key words:** Bentonite, deep geological repository, sulfate-reducing bacteria, rare
40 biosphere, long-term incubation, microbial inhibition, radioactive waste disposal,
41 Opalinus Clay rock

42

43 **Introduction**

44 Deep geological repositories (DGRs) will host high-level radioactive waste primarily
45 from nuclear power plants. Bentonite clay is considered in some disposal concepts as
46 one of the engineered barriers in the multibarrier system of DGRs [1]. It will be placed
47 around the disposal canister in the emplacement drift, filling the gap between the
48 canister and the host rock, in a process referred to as backfilling. In the case of the
49 Swiss concept, bentonite ensures waste isolation by mechanically protecting the
50 canister, and by combining sorption capacity with swelling pressure—properties that
51 retain radionuclides after canister breach (expected after more than 10,000 years) [2–
52 4]. It complements the radionuclide retention effect of the clay-rich host rock formation,
53 Opalinus Clay.

54 However, bentonite backfill introduces microorganisms, in addition to those already
55 present in the host rock and those introduced by operations [5–8]. These
56 microorganisms possess diverse metabolic traits that can become active as repository
57 conditions evolve from partly saturated and oxic to fully saturated and anoxic. Sulfate
58 (SO_4^{2-}) reduction is of particular concern, as hydrogen sulfide (HS^-) produced by
59 sulfate-reducing bacteria (SRB) may accelerate canister corrosion once oxygen (O_2)
60 is depleted. In addition, microbial activity shapes gas turnover, particularly hydrogen
61 (H_2) and methane (CH_4), with implications for gas buildup that must be reliably
62 predicted to ensure repository safety [9]. To restrict microbial activity, strategies like
63 compacting bentonite clay to high densities (for example, 1.45 g/cm^3 for Wyoming
64 bentonite) have been suggested. This approach controls pore space, pressure, water
65 activity, and substrate diffusion rates, all of which are critical controls for the

66 proliferation of microbes [10, 11]. Yet, predicting microbial survival and activity over of
67 thousands to hundreds of thousands of years remains a major challenge.

68 Long-term laboratory and *in-situ* incubation studies on compacted bentonite have
69 therefore become key to understanding microbial fate. Results from previous studies
70 conducted after 1–8 years of incubation [12–17] indicate that: (i) microbial cell
71 numbers remain stable or decline is minimal, (ii) colonization from host rock and/or
72 porewater is limited and bentonite communities alone show little temporal change, (iii)
73 compaction is the dominant control on abundance and diversity, and (iv) irrespective
74 of incubation length or density, part of the indigenous microbiota remains alive and
75 can be revived by cultivation. Strikingly, across all studies, viable aerobic heterotrophs
76 consistently outnumber culturable anaerobes, and (facultatively) aerobic bacteria like
77 *Streptomyces* spp. and *Pseudomonas* spp. are frequently found in high abundance in
78 the sequencing datasets. Burzan et al. (2022) proposed that this paradox can be
79 explained by slow desorption and dissolution of O₂ from bentonite, which sustains
80 aerobic metabolism while suppressing anaerobic activity [12]. Whether aerobes
81 eventually decline once O₂ is consumed, allowing anaerobes such as SRB to expand,
82 or whether bentonite compaction continues to inhibit the entire community remains
83 unresolved.

84 Here, we provide a unique continuous *in-situ* dataset from Wyoming bentonite
85 incubation in the same Opalinus Clay borehole for 1.5, 5.5, and 8.5 years, providing
86 robust temporal comparisons over long timescales. By combining cultivation-based
87 enumerations with cultivation-independent 16S rRNA sequencing, we focus on
88 patterns of aerobe persistence and the potential emergence of anaerobic metabolism
89 under repository-like conditions. We further test how time, bentonite density (1.25,

90 1.45, 1.55 g/cm³) and formulation (bentonite blocks vs. pellets) shape microbial
91 community structure and fate. Together, these data help refine long-term predictions
92 of microbial impact on barrier performance in DGRs.

93 **Materials and Methods**

94 **Experimental design and module assembly.** Experimental modules consisted of
95 stainless-steel cylinders (25 cm height, 12.6 cm outer diameter) lined with a sintered
96 porous stainless-steel filter and filled with Wyoming bentonite at one of three dry
97 densities and one of two bentonite formulations: 1.25 g/cm³ (pre-compacted blocks),
98 1.45 g/cm³ (pellets), and 1.55 g/cm³ (pre-compacted blocks). Modules containing
99 pellets were saturated with anoxic deionized water and placed under vacuum during
100 compaction to minimize residual oxygen. Blocks were handled and stored under 100%
101 N₂ until assembly, after which they were similarly saturated. In addition, all modules
102 contained metallic coupons embedded within bentonite for corrosion analysis (not
103 covered here). Modules were deployed for 8.5 years in an anoxic, porewater-filled
104 borehole in the Opalinus Clay at the Mont Terri Rock Laboratory (St-Ursanne,
105 Switzerland). Results from this phase are compared with previously published data
106 from the same borehole, including as-received bentonite and bentonite incubated for
107 1.5 or 5.5 years. The analysis focuses on the two most recent time points (5.5 and 8.5
108 years), while earlier data are included where relevant for context. Detailed analyses of
109 earlier time points are available in the published literature [12, 18].

110 **Bentonite sampling.** After removal from the borehole, the modules were immediately
111 packed under anoxic conditions (100% N₂), transported to the laboratory, and stored
112 at 4 °C. In an anoxic glovebox (100% N₂), the porous filters were removed from the
113 modules and cut along the module axis to access bentonite. Bentonite was then

114 sectioned using sterile tools following established protocols used in the previous
115 phases of the Iron Corrosion (IC-A) Experiment [12]. Sections were separated and
116 preserved at 100% Ar and 4 °C for analysis of water content, clay density, microbial
117 community and for microbial cultivation. Later, the samples were further subsampled
118 to isolate the outer (at the interface with the borehole surface) and inner core fractions.
119 After subsampling, the outer and inner parts were either used for cultivation studies,
120 in which case they were stored anoxically at 4 °C, or for gDNA enumeration and
121 sequencing, with preservation at -20°C.

122 **Microbial cultivation.** Heterotrophic aerobes and anaerobes were enumerated in
123 triplicate from anoxically prepared bentonite suspensions using a consistent approach
124 across all time points. The semi-solid pour plate method was used with R2A medium
125 [21]: liquid agar medium was cooled down to 45–50°C and grown under oxic (3 days)
126 or anoxic (30 days) conditions at 30°C. The enumeration of SRB was performed with
127 the most probable number (MPN) method [22]. Hungate tubes were filled with 9 ml of
128 sterile, anoxic Postgate's Medium B (Medium 63: Desulfovibrio (Postgate) Medium,
129 2022) and serial dilutions from 10⁻¹ to 10⁻⁵ were made (in triplicates) using the same
130 inoculum as for heterotrophic anaerobes and aerobes. The tubes were sealed to
131 maintain anoxic conditions during 7 weeks of incubation at 30°C.

132 **DNA extractions and sequencing.** DNA was extracted following methods described
133 by [24] utilizing a modified protocol of DNeasy PowerMax Soil Kit (QIAGEN NV, Venlo,
134 The Netherlands). Bentonite DNA was additionally purified by using 10 μ L
135 Invitrogen™ Linear Acrylamide (5 mg/mL), 0.1 volume of 5 M NaCl and 2 volumes of
136 isopropanol. The air-dried DNA pellets were resuspended in 40 μ L elution buffer
137 provided in the DNeasy® PowerMax® Soil Kit and stored at -20°C. Extracted DNA
138 was quantified using an Invitrogen Qubit 2.0 fluorometer with 2 μ L of extracted DNA
139 and 198 μ L of working solution prepared by mixing Qubit™ buffer solution and
140 fluorescent Qubit™ reagent following the standard protocol provided by the
141 manufacturer. Sequencing was performed targeting 16S rRNA gene V4 region with
142 library prepared using Quick-16S Plus NGS Library Prep Kit (V4) from Zymo (DS6430)
143 at using Miseq v2 PE150 platform.

144 **16S rRNA gene copy quantification.** Quantitative PCR (qPCR) analysis of the
145 bacterial and archaean 16S rRNA gene was performed using the MYRA robotic
146 system and a MIC qPCR Cycler (both BioMolecular Systems, Australia). Analyses
147 were carried out in triplicate in 10 μ L reactions. For quantification of the gene
148 abundance, the following volumes of substrates were used: 2.5 μ L template DNA, 2.1
149 μ L water, 0.2 μ L of each primer (100 mM stock) and 5 μ L of 2 \times SensiFAST SYBR[®]
150 No-ROX Kit (Meridian Bioscience, UK). Samples were cycled (40 cycles) at 95 $^{\circ}$ C for
151 5 s, followed by an extension at 62 $^{\circ}$ C for 10 s and the acquisition at 72 $^{\circ}$ C for 5 s. The
152 final melting step was carried out from 72 $^{\circ}$ C to 95 $^{\circ}$ C, at a rate of 0.1 $^{\circ}$ C/s. Analysis
153 of the results was performed using the built-in analytical software (micPCR,
154 BioMolecular Systems, ver. 2.12.6). Average efficiency (0.943 – 1.003) and r^2 values
155 (> 0.99) were determined from seven points of the serial dilutions (10^7 – 10^1 copies)
156 for bacterial 16S rRNA gene. Based on calibration curves obtained using *E. coli* DNA,
157 C_q values were used to calculate the gene copy numbers which were normalized
158 against mass (ng) of the extracted DNA. The primer pair used for the reaction to
159 quantify bacterial 16S rRNA gene consisted of 338f: 5'-ACT CCT ACG GGA GGC
160 AGC AG-3' and 534r: 5'-ATT ACC GCG GCT GCT GGC A-3'.

161 **Bioinformatic analysis.** The multiplexing barcodes were removed and raw sequence
162 read quality was assessed using FastQC [25]. The reads were then processed in the
163 R (version 4.5.2) [26] package dada2 [27]. Forward 'AGRGTTYGATYMTGGCTCAG'
164 and reverse 'RGYTACCTTGTTACGACTT' primers were removed. After filtering and
165 dereplication, error rates were learned to denoise the reads and obtain Amplicon
166 Sequence Variants (ASVs). Taxonomy of ASVs was determined using the SILVA
167 database (released 138.1) formatted to be compatible with dada2 and the RDP Naive

168 Bayesian Classifier algorithm [28, 29]. Chimeras were detected and removed for
169 subsequent analysis. PCoA was based on Bray-Curtis dissimilarity (*vegdist*,
170 *cmdscale*; *vegan*), and RDA was performed using *rda* with significance assessed by
171 permutation tests (*anova.cca*) [30]. The R package *ulrb* was used to define the rare
172 biosphere in the samples by comparing ASV abundances and clustering them into
173 three relative categories: 'rare', 'abundant', and 'undetermined', which avoids using
174 arbitrary abundance thresholds [31]. Functional profiles were predicted from 16S rRNA
175 gene data using PICRUSt2 [32]. Data processing was performed using *dplyr* and *tidyr*,
176 and figures were generated with *ggplot2* [33, 34].

177 **Bentonite water content and dry density determination.** Water content was
178 calculated by obtaining the bentonite wet and dry mass after 24h in an oven at 105°C
179 and reported in Figure S1 and **Table S1**.

180 **Statistical analysis.** Analysis of Variance (ANOVA) at a significance level (alpha) of
181 0.05, was used to discern significant differences between the treatments. In instances
182 for which the ANOVA indicated that significant differences existed within data sets,
183 pairwise comparisons were conducted using the t-Student test for each pair at a
184 significance level (alpha), adjusted for multiple comparisons using the Bonferroni
185 correction method.

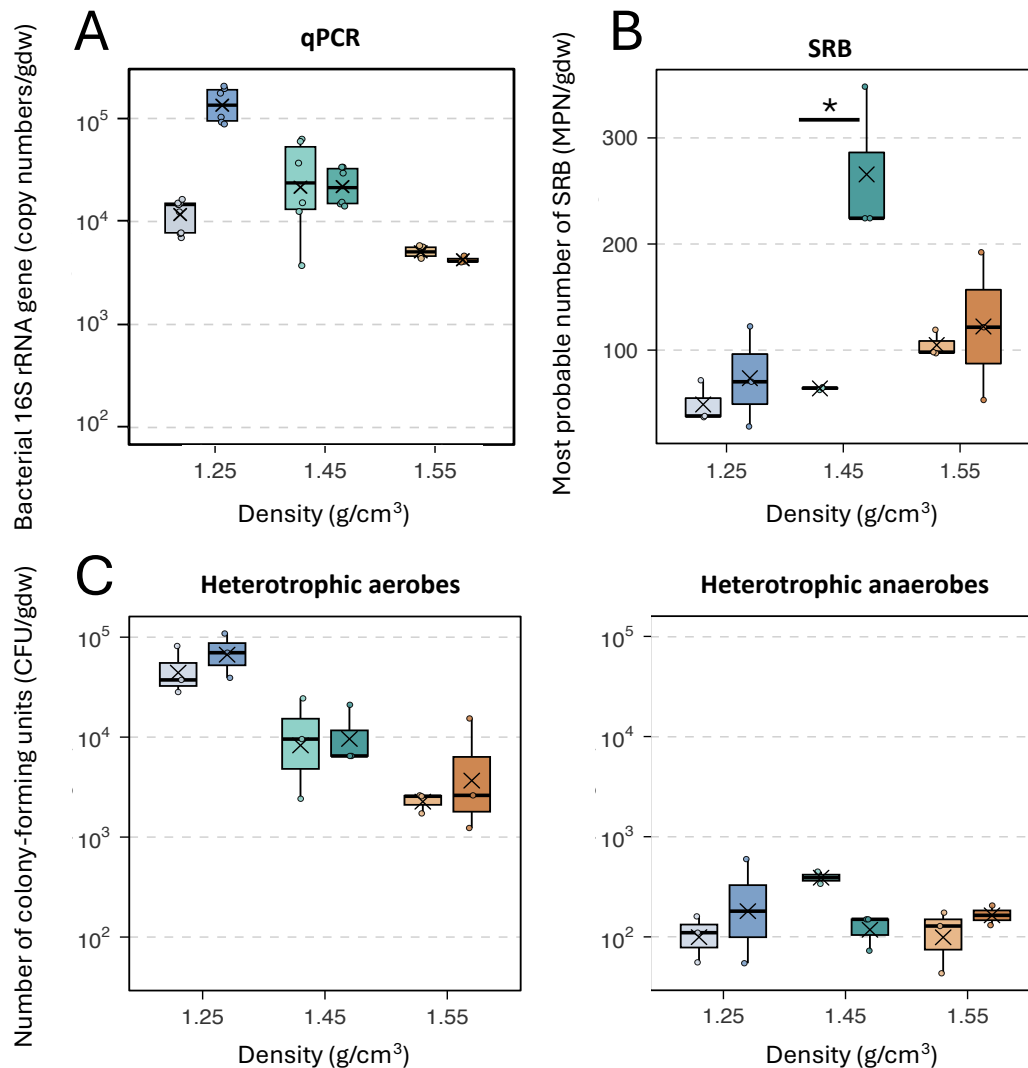
186 **Results and Discussion**

187 *Microorganisms remain viable and cultivable after 8.5 years in compacted bentonite*
188 After 8.5 years of *in-situ* incubation, microorganisms remained detectable and, in part,
189 viable across all bentonite densities. Quantitative PCR confirmed the presence of
190 bacterial and archaeal 16S rRNA genes in all samples, with abundances overall

191 decreasing systematically and significantly with increasing dry density (ANOVA,
192 $p=0.05$) (**Figures 1A, S2**). This inverse relationship confirms that compaction is a
193 strong constraint on microbial persistence. Significant differences in bacterial cell
194 numbers (pairwise t-student, $p=0.05$) between the outer layer and the inner part of
195 bentonite were observed only for the bentonite at the lowest density (1.25 g/cm^3).
196 Despite long-term energy-limiting conditions, cultivable anaerobic and aerobic
197 heterotrophic microorganisms were still recoverable. In general, the number of colony-
198 forming units (CFU) followed the same trend as 16S rRNA gene copy numbers: the
199 lower the dry density, the higher the number of CFU. No statistical difference was
200 shown between the outer and inner parts of the core at any of the densities (pairwise
201 t-student tests, $p=0.05$). CFU numbers of anaerobes were on average two orders of
202 magnitude lower than those of aerobes. Similarly to aerobes, there was no statistical
203 difference between the outer parts of the core and inner parts in terms of CFU
204 numbers. The average numbers, together with standard deviations for both aerobes
205 and anaerobes (CFUs) are presented in **Table S2**.

206

207



208

209 **Figure 1. Microbial abundance and viability in bentonite after 8.5 years of incubation.**
 210 For each dry density, inner core samples are shown in the left box and outer core samples in
 211 the right box. **(A)** 16S rRNA gene copy numbers per gram dry weight (gdw) determined by
 212 qPCR after 8.5 years of borehole incubation. **(B)** Sulfate-reducing bacteria viability determined
 213 by MPN counts (linear scale). **(C)** Number of colony-forming units (CFU) of heterotrophic
 214 aerobes and anaerobes (log₁₀ scale). Colors indicate bentonite density (1.25, 1.45, and 1.55
 215 g/cm) and sample position. Boxes show the interquartile range (IQR), the line indicates the
 216 median, whiskers extend to 1.5× IQR, crosses show the mean, and points represent individual
 217 samples. Asterisks indicate significant differences (*p < 0.05).

218

219 The large difference in cultivable aerobes and anaerobes has been previously
 220 reported in other long-term *in-situ* incubation experiments [12, 17] and suggests that
 221 at least some of the aerobes found in bentonite incubated under anoxic conditions for
 222 8.5 years are obligate aerobes. If this were not the case, the cultivation on the anoxic
 223 medium should result in higher CFU counts, supporting both obligate and facultative

224 anaerobes. Further, this suggests that either the viable aerobes persist in compacted
225 bentonite in a dormant state, without active growth, or that even after 8.5 years, they
226 are still at least partially supported by residual oxygen as previously described [12,
227 35].

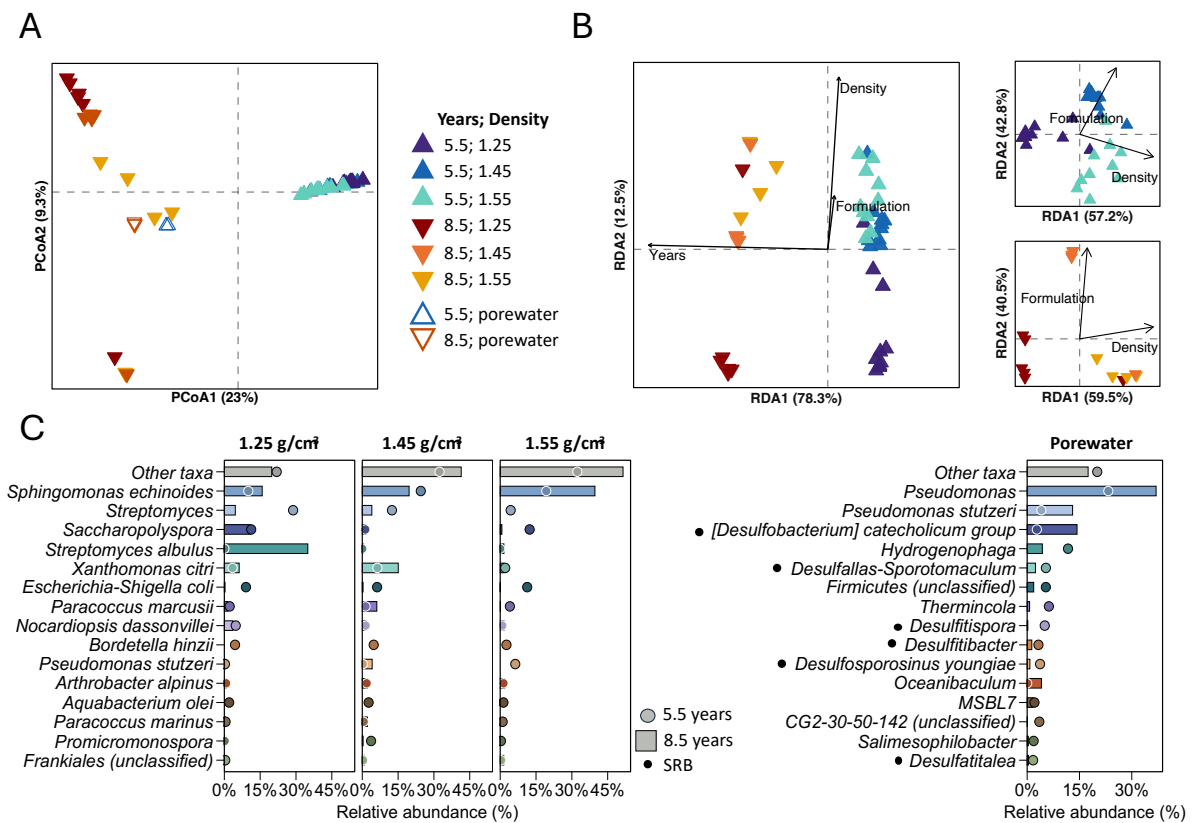
228 Cultivable sulfate-reducing bacteria (SRB) were detected in all bentonite cores after
229 8.5 years of incubation. No consistent relationship was observed between SRB
230 abundance and bentonite density. In the outer core, the difference between the lowest
231 (1.25 g/cm^3 ; $73.5 \pm 47.3 \text{ MPN g}^{-1}\text{dw}$) and highest density (1.55 g/cm^3 ; 122.3 ± 69.6
232 $\text{MPN g}^{-1}\text{dw}$) was not significant, whereas the 1.45 g/cm^3 module showed significantly
233 higher values ($265.6 \pm 71.7 \text{ MPN g}^{-1}\text{dw}$). This indicates that bentonite formulation
234 (blocks vs. pellets), rather than density alone, might play a more important role in SRB
235 presence and survival. Except for the 1.45 g/cm^3 case, no significant differences were
236 observed between outer and inner core samples.

237 Across both cultivation-dependent and -independent assays, slightly higher
238 abundances were often detected in the outer parts, but these differences were
239 generally not significant. This suggests that small-scale spatial gradients within the
240 cores are negligible. Therefore, for consistency with previous studies, outer and inner
241 samples are averaged in the rest of the manuscript when compared with previous time
242 points.

243 *Time is the dominant driver of long-term microbial community change*

244 Ordination analyses based on 16S rRNA gene sequencing data indicated that
245 incubation time was the primary driver of bentonite community composition. PCoA
246 demonstrated a strong separation between 5.5-year and 8.5-year samples (**Figure**
247 **2A**). An RDA showed that time explained approximately 78% of the total variance for

248 bentonite samples (**Figure 2A, B**), while borehole porewater communities remained
 249 similar (**Figure 2B**). This temporal change was far more explanatory than density or
 250 formulation (**Figure 2B**). These results suggest that microbial communities in
 251 compacted bentonite change slowly but persistently over nearly a decade, even under,
 252 and perhaps in response to, extreme nutrient and physical limitations. After accounting
 253 for the strong temporal effect, density was shown to be the main factor influencing
 254 community composition at each time point (**Figure 2B**). The impact of formulation
 255 (block vs. pellet) could not be fully determined due to limited replication, as only one
 256 density was tested in the block form. Overall, these findings suggest that bentonite
 257 density initially structures microbial community composition, after which temporal
 258 effects become increasingly dominant, driving stronger divergence over time (5.5 and
 259 8.5 years).



260

261 **Figure 2. Microbial community structure and dynamics in compacted bentonite and porewater.**
262 **(A)** PCoA of microbial community composition based on 16S rRNA gene sequencing data. **(B)** RDA of
263 bentonite samples illustrating the influence of dry density and incubation time on community structure.
264 The three subpanels correspond to all samples (left), 5.5 years (top right) and 8.5 years (bottom right).
265 **(C)** Relative abundance of the 15 most abundant bacterial taxa across bentonite densities (1.25, 1.45,
266 and 1.55 g/cm³) and porewater; dots indicate 5.5-year samples and bars indicate 8.5-year samples.

267

268 *Bentonite and borehole porewater host distinct microbial communities*

269 To identify which microbial species are changing in abundance over time, the
270 communities were sorted by the 15 most abundant microorganisms in bentonite and
271 in porewater, all bacteria. Among all bentonite samples, a small set of taxa dominated
272 the bentonite microbiome, including *Sphingomonas*, *Streptomyces*,
273 *Saccharopolyspora*, *Xanthomonas*, and *Nocardiopsis spp.*, previously identified as the
274 core bentonite microbiome [8] (**Figure 2C**). These taxa are characterized by
275 adaptation to extreme environments via metabolic versatility, stress tolerance, and in
276 some cases, spore formation, and oligotrophy [36–42].

277 Relative to the earlier sampling (5.5-year time point), density-dependent trends were
278 observed, with *Sphingomonas* and *Streptomyces albulus* increasing at 1.25 g/cm³. At
279 1.45 g/cm³, *Paracoccus* and *Pseudomonas stutzeri* became more dominant. At 1.55
280 g/cm³, most taxa declined, except for *Streptomyces echinoides*, suggesting that time
281 selects for a narrow set of highly resilient organisms. In terms of absolute abundance,
282 consistent with the overall decline in total 16S rRNA gene copy numbers, all taxa
283 decreased after 8.5 years of incubation compared to 5.5 years, regardless of bentonite
284 density. The only exception was *Streptomyces albulus*, which increased to 2.26×10^4
285 16S rRNA gene copies at a density of 1.25 g/cm³, making it the most abundant
286 microorganism in all bentonite samples after 8.5 years (**Figure S3**; see SI for further
287 discussion). Archaea were also detected in bentonite samples after 8.5 years but did

288 not exceed 0.3% of the total relative abundance, except in samples collected from the
289 interior of module M8 (1.55 g/cm³, blocks), where they accounted for 3.8% of the
290 overall microbial community. Details and discussion of archaeal community
291 composition are provided in the SI.

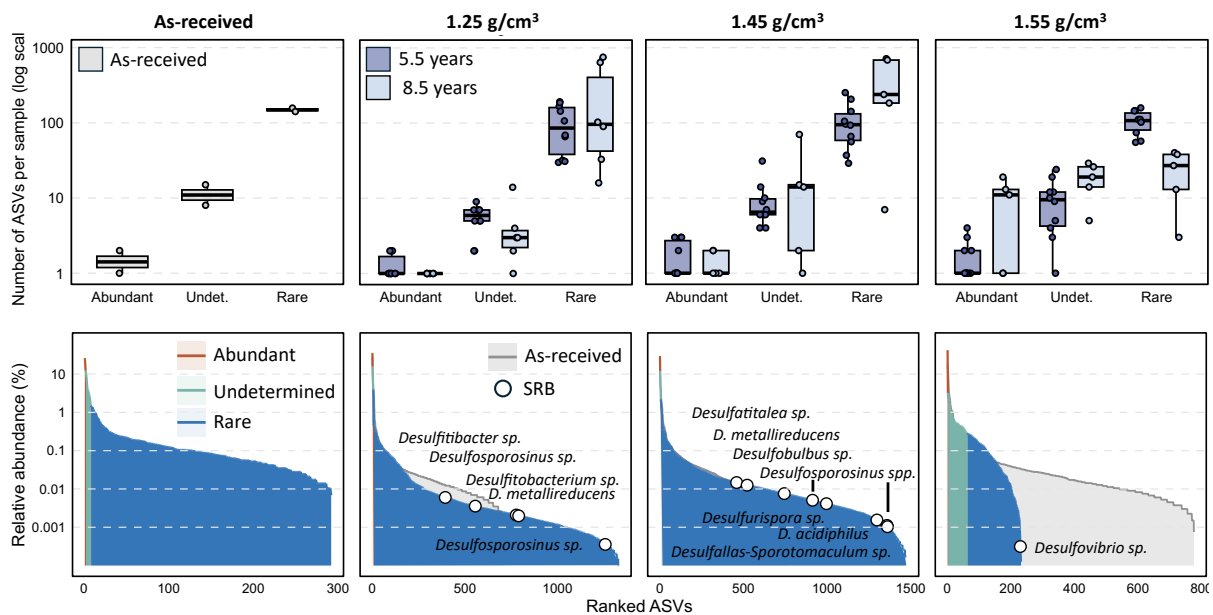
292 The porewater showed a distinct taxonomic composition to that of the bentonite-
293 associated communities. It was dominated by two *Pseudomonas* spp. and by taxa
294 commonly classified as sulfate-reducing bacteria (SRB), which accounted for 21.6 ±
295 0.77% of the community at the time of module retrieval after 8.5 years of incubation
296 (**Figure 2C**). Some SRB lineages, such as the *Desulfobacterium catecholicum* group,
297 increased over time (from 2.78 ± 0.72 to 14.31 ± 1.39). Other SRB among the 15 most
298 abundant porewater taxa included members of the *Desulfallas–Sporotomaculum*
299 group, *Desulfosporosinus youngiae*, and *Desulfatitalea* spp.. Other sulfidogens, the
300 sulfite reducers *Desulfitispora* and *Desulfitibacter*, were also prominent in the
301 community.

302 Despite the long incubation time of the bentonite in the borehole, there was remarkably
303 little taxonomic overlap between the borehole porewater and the bentonite
304 communities. This indicates a very limited capacity of borehole microorganisms to
305 colonize the compacted bentonite matrix, even after nearly a decade of physical
306 contact. This observation is consistent with previous long-term *in-situ* studies in the
307 same borehole [12] and with recent work showing that porewater-derived
308 microorganisms penetrate only the outermost ~1 cm of the compacted bentonite [35].

309 *Sulfate reducers persist as a rare biosphere in bentonite*

310 Because the bentonite community is dominated by low-abundance taxa, we analyzed
311 community structure using rank abundance. Taxa were classified into categories

312 based on their relative abundance across samples, defining abundant, intermediate
 313 (undetermined), and rare fractions (see Methods). This classification allowed us to
 314 assess whether sulfate-reducing bacteria (SRB) preferentially occur within specific
 315 abundance fractions and how this distribution may change over time and across
 316 densities.



317

318 **Figure 3. Unsupervised learning-based classification of the bentonite microbiome into**
 319 **abundant, rare, and undetermined populations.** Top three panels: boxplots showing the number of
 320 abundant, rare and undetermined ASVs for each incubation duration (5.5 or 8.5 years) and across dry
 321 densities: boxes show the interquartile range (IQR), the line indicates the median, whiskers extend to
 322 1.5× IQR, crosses show the mean, and points represent outliers. Bottom three panels: rank abundance
 323 plots comparing as-received bentonite to community distribution after 8.5 years of incubation. SRB that
 324 were only detected at 8.5 years are highlighted with white circles.

325

326 At low and intermediate densities (1.25 and 1.45 g/cm³), the relative contribution of
 327 rare taxa increased over time, while at high density (1.55 g/cm³), the rare fraction
 328 declined (**Figure 3**). One possible explanation for the apparent increase in the rare
 329 fraction is the gradual loss of previously abundant or undetermined taxa, which would
 330 cause them to fall into the rare category. However, this occurrence alone cannot fully
 331 explain the observed patterns, because abundant and undetermined taxa together

332 represent only a small fraction of the total community (approximately 10–100 out of
333 ~1000 ASVs). Instead, the pattern could be explained by the emergence of slow
334 growing, highly specialized microorganisms that were initially below detection.
335 Conversely, the sharp decline of rare taxa at 1.55 g/cm³ indicates that even these
336 specialists are unable to persist at high compaction. This suggests that a critical
337 density threshold between 1.45 and 1.55 g/cm³ strongly limits microbial survival and
338 leads to the decline of the rare biosphere.

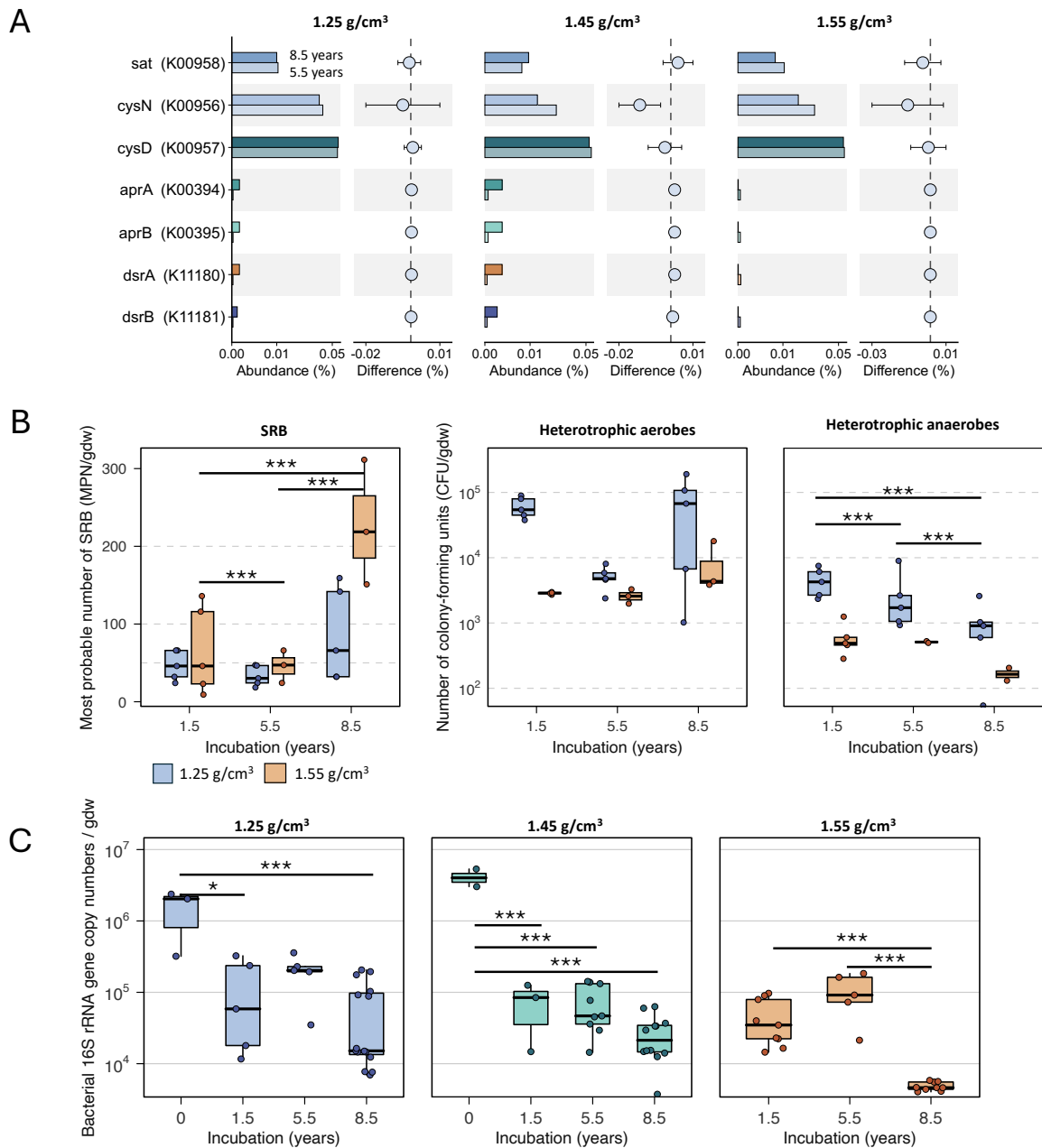
339 At all three densities, taxonomically identified SRB-related taxa were exclusively found
340 within the rare biosphere ($\leq 0.01\%$ relative abundance), with the highest **(Figure S4)**
341 in the 1.45 g/cm³ case. At 1.55 g/cm³, only a single SRB-related species, *Desulfovibrio*
342 *sp.*, was identified. Notably, SRB-related taxa were observed only in bentonite that
343 had been incubated in the borehole and were absent from the as-received bentonite
344 prior to incubation. This suggests that these SRB are either introduced from the
345 surrounding porewater and subsequently migrate into the bentonite, though their
346 migration is spatially limited [35], or more likely, are initially present in the bentonite at
347 low abundances and become detectable only under borehole incubation conditions.
348 However, their consistently low relative abundance, particularly at high dry density,
349 indicates that while borehole conditions may support their persistence, the compacted
350 bentonite matrix strongly suppresses their growth.

351 To assess how the sulfate reduction potential evolves over time, we used metabolic
352 predictions derived from taxonomic data. PICRUST2 analysis revealed no significant
353 changes in the predicted abundance of genes related to sulfate reduction **(Figure 4A)**
354 between 5.5 and 8.5 years. Consistent with this result, SRB MPN cultivation results
355 **(Figure 4B)** showed no statistically significant temporal changes at 1.25 g/cm³ across

356 the compared timepoints (1.5–5.5–8.5 years). In contrast, at 1.55 g/cm³ (that has the
357 same block formulation), a significant increase in SRB MPN counts was observed over
358 time, indicating a selective advantage for the small subset of microorganisms capable
359 of sulfate reduction, that persist and grow under conducive cultivation conditions. Note
360 that the Postgate medium used for MPN was originally optimized for *Desulfovibrio*
361 *desulfuricans* as a model SRB species [43], and because *Desulfovibrio sp.* were the
362 only SRB detected at density of 1.55 g/cm³, they likely benefited both from reduced
363 competition and from growth conditions designed for this group. None of the other
364 metabolic groups tested in cultivation, including heterotrophic anaerobes and aerobes,
365 showed a similar response at 1.55 g/cm³, with revived populations remaining stable
366 (aerobes) or declining (anaerobes) (**Figure 4B**). This decoupling between abundance,
367 diversity, and cultivability highlights the importance of monitoring rare taxa, which may
368 carry the potential for critical processes such as sulfate reduction.

369

370



371

372 **Figure 4. Temporal changes in sulfate reduction potential, microbial viability, and**
 373 **microbial abundance in compacted bentonite.**

374
 375 **(A)** PICRUSt2 predictions of genes associated with sulfate reduction in bentonite samples
 376 after 5.5 (lower bar) and 8.5 (upper bar) years of incubation for the three densities. **(B)**
 377 Cultivation-based most probable number (MPN) estimates of sulfate-reducing bacteria (SRB),
 378 aerobic heterotrophs, and anaerobic heterotrophs at 5.5 and 8.5 years. Note that for the
 379 density of 1.45 g/cm³, complete cultivation data from earlier time points are unavailable and
 380 therefore not included in the comparison. **(C)** Bacterial 16S rRNA gene copy numbers
 381 determined by qPCR for as-received bentonite and after 1.5, 5.5, and 8.5 years of *in-situ*
 382 incubation.

383

384 *Overall microbial abundance and activity decline over time*

385 A comparison of 16S rRNA gene copy numbers throughout all experimental phases
386 (**Figure 4C**) revealed that gene copies quantified after 8.5 years of incubation are
387 significantly lower (pairwise t-student, <0.05 ; **Table S3**) when compared to available
388 reference materials before the deployment into the borehole and, in case of the most
389 compacted bentonite, the 1.55 g/cm^3 case, also are significantly lower when compared
390 to the last sampling point after 5.5 years of incubation. The decrease indicates
391 bacterial death, but also the possible degradation of extracellular DNA (eDNA) that
392 was initially present in the as-received bentonite but did not correspond to living cells.
393 A decrease in the cultivability of anaerobic heterotrophs relative to previous time points
394 further supports bacterial death over the years of incubation. Together, these results
395 indicate a progressive loss of viable microbial biomass under bentonite confinement,
396 particularly under the highest density compaction.

397 The microbial population data presented here, together with earlier time points from
398 the same Opalinus Clay borehole at the Mont Terri Rock Laboratory [12], show a
399 different pattern from that observed in a parallel experiment in granitic rock at the
400 Grimsel Test Site. In an Opalinus Clay borehole, microbial abundance in bentonite
401 declined after 1 year and continued to decrease over 5.5 and 8.5 years, whereas the
402 microbial populations in bentonite in a Grimsel Test Site borehole remained stable
403 over 1, 5 and 7 years [13, 14, 16]. This contrast may reflect differences in porewater
404 chemistry. Opalinus Clay borehole water has circumneutral pH, high sulfate
405 concentration but also high ionic strength (pH $\sim 7.2\text{--}7.6$, $\sim 0.3\text{--}0.4 \text{ mol L}^{-1}$ ionic
406 strength, $\text{SO}_4^{2-} \sim 10\text{--}25 \text{ mmol L}^{-1}$)[44], whereas Grimsel borehole water has higher pH
407 ($\sim 9\text{--}9.5$), low sulfate ($\sim 0.06 \text{ mmol L}^{-1}$) and low ionic strength ($\sim 10^{-3} \text{ mol L}^{-1}$)[45]. The

408 higher ionic strength corresponding to higher salinity may create stronger osmotic
409 stress, potentially causing the observed decline. Except for the differences in
410 abundance, both *in-situ* experiments show similar results: taxa typically classified as
411 aerobic remain dominant despite anoxic conditions, while SRB can be cultivated after
412 7–8.5 years but remain a minor component of the community.

413

414 *Conclusion and implications for the long-term performance of geological repositories*

415 Our 8.5-year-long incubation experiment demonstrated that the microbial inhibition in
416 underground repositories using bentonite as a backfill material is effective. For all
417 tested bentonite buffer densities , microbial cell numbers remain low and generally
418 decline over time, with dry density emerging as the dominant control on microbial
419 persistence.

420 At the lowest tested dry density (1.25 g/cm³), microbial abundances were initially
421 higher than at the more compacted densities. Nevertheless, no overall population
422 increase was observed; instead, microbial numbers steadily declined throughout the
423 experiment. These findings indicate that Wyoming bentonite compacted to 1.25 g/cm³,
424 which is below the often-proposed target repository density of 1.45 g/cm³, is sufficient
425 to prevent sustained microbial growth and serves as an effective biological barrier. At
426 higher densities (≥ 1.55 g/cm³), both microbial abundance and diversity were strongly
427 limited, including within the rare biosphere, suggesting the existence of a density
428 threshold above which even highly specialized and slow-growing microorganisms
429 cannot persist.

430 Importantly, sulfate-reducing bacteria (SRB), although recoverable in cultivation
431 assays, did not increase in relative abundance in the community over time and

432 remained confined to the rare biosphere. This decoupling between cultivability and *in-*
433 *situ* abundance indicates that SRB persistence reflects survival rather than actual
434 growth, limiting concerns about the progressive enrichment of corrosion-inducing
435 microorganisms within the bentonite due to developing anoxic conditions. In addition,
436 the bentonite barrier effectively limited the colonization of borehole microorganisms,
437 which is particularly relevant given that the surrounding porewater community contains
438 a substantial fraction of SRB (up to 22%). This confirms that bentonite acts not only
439 as a physical and geochemical barrier but also as an effective biological isolation
440 barrier.

441 The detection of methanogenic archaea reaching up to 3.8% relative abundance
442 highlights that certain anaerobic metabolic pathways can persist and even slowly
443 emerge under repository-relevant conditions, suggesting that methane production
444 cannot be excluded over very long timescales. However, the low absolute abundances
445 and strong density dependence indicate that such processes are likely to remain
446 spatially constrained.

447 Finally, the persistence of aerobic heterotrophs, despite long-term anoxic conditions,
448 shows the importance of dormancy, metabolic flexibility, and maintenance energy
449 strategies for microbial survival in compacted bentonite, and confirms that residual
450 oxygen and redox niches may persist over longer timescales than often assumed.

451 Overall, our findings indicate that density is the primary factor shaping microbial
452 communities in bentonite, while time becomes important at long temporal scales,
453 driving further gradual changes. The communities that persist are characterized by
454 low abundance, high specialization, and restricted function. Together, these
455 processes lead to a progressive decline in microbial abundance and activity,

456 supporting the long-term effectiveness of Wyoming bentonite as a biological barrier in
457 deep geological repositories.

458 **Data availability statement**

459
460 Raw DNA sequence data underlying this article are available in Zenodo repository
461 under DOI <https://doi.org/10.5281/zenodo.4883717> for the 1.5- and 5.5-year time
462 points and under DOI <https://doi.org/10.5281/zenodo.20964472> for the 8.5-year time
463 point.

464

465 **Acknowledgements**

466 Niels Burzan, Manon Frutschi, Solexperts AG, Nagra and the Mont Terri Project Team
467 are acknowledged for their fieldwork support during modules retrieval. Thanks to
468 Nicolas Jacquemin for processing bioinformatics data and Pierre Rossi and EPFL
469 Central Environmental Laboratory for qPCR results. Basile Tornare helped with
470 microbial cultivation and enumeration. Following the Permitted Uses of LLMs,
471 Grammarly was used to correct written text (spellcheckers and grammar checkers).

472

473

474

475 **References**

476

- 477 1. Status and Trends in Spent Fuel and Radioactive Waste Management. 2025.
- 478 2. Design and performance assessment of HLW disposal canisters. NTB 24-20.
479 *Nagra Technical Report 2024*; **NTB 24-20**.
- 480 3. Diomidis N, Johnson LH. Materials Options and Corrosion-Related
481 Considerations in the Design of Spent Fuel and High-Level Waste Disposal
482 Canisters for a Deep Geological Repository in Opalinus Clay. *JOM* 2014 66:3
483 2014; **66**:461–470. <https://doi.org/10.1007/S11837-014-0876-4>
- 484 4. Patel R et al. Canister design concepts for disposal of spent fuel and high level
485 waste. 2012.
- 486 5. Stroes-Gascoyne S. Microbial occurrence in bentonite-based buffer, backfill
487 and sealing materials from large-scale experiments at AECL's Underground

- 488 Research Laboratory. *Appl Clay Sci* 2010;**47**:36–42.
489 <https://doi.org/10.1016/j.clay.2008.07.022>
- 490 6. Mitzscherling J et al. Clay-associated microbial communities and their
491 relevance for a nuclear waste repository in the Opalinus Clay rock formation.
492 *Microbiologyopen* 2023;**12**:e1370. <https://doi.org/10.1002/MBO3.1370>.
- 493 7. Stroes-Gascoyne S et al. Microbial community analysis of Opalinus Clay drill
494 core samples from the Mont Terri Underground Research Laboratory,
495 Switzerland. *Geomicrobiol J* 2007;**24**:1–17.
496 <https://doi.org/10.1080/01490450601134275>
- 497 8. Vachon MA et al. Fifteen shades of clay: distinct microbial community profiles
498 obtained from bentonite samples by cultivation and direct nucleic acid
499 extraction. *Sci Rep* 2021;**11**:1–13. <https://doi.org/10.1038/s41598-021-01072-1>
- 500 9. Leupin OX et al. Fifteen years of microbiological investigation in Opalinus Clay
501 at the Mont Terri rock laboratory (Switzerland). *Swiss J Geosci* 2017;**110**:343–
502 354. <https://doi.org/10.1007/s00015-016-0255-y>
- 503 10. Beaver RC et al. Interface-associated microbial growth in anoxic pressure
504 vessels containing compacted gapfill bentonite. *J Appl Microbiol* 2025;**136**:157.
505 <https://doi.org/10.1093/JAMBIO/LXAF157>
- 506 11. Sellin P, Leupin OX. The Use of Clay as an Engineered Barrier in Radioactive-
507 Waste Management a Review. *Clays and Clay Minerals* 2013 **61**:6
508 2013;**61**:477–498. <https://doi.org/10.1346/CCMN.2013.0610601>
- 509 12. Burzan N et al. Growth and Persistence of an Aerobic Microbial Community in
510 Wyoming Bentonite MX-80 Despite Anoxic in situ Conditions. *Front Microbiol*
511 2022;**13**:1–12. <https://doi.org/10.3389/fmicb.2022.858324>
- 512 13. Engel K et al. Stability of Microbial Community Profiles Associated with
513 Compacted Bentonite from the Grimsel Underground Research Laboratory.
514 2019. <https://doi.org/10.1128/mSphere>
- 515 14. Engel K et al. Stable microbial community in compacted bentonite after 5 years
516 of exposure to natural granitic groundwater. *mSphere* 2023;**8**.
517 <https://doi.org/10.1128/MSPHERE.00048-23>
- 518 15. Povedano-Priego C et al. Indigenous bacterial adaptation and survival:
519 Exploring the shifts in highly compacted bentonite over a 5-year long-term
520 study for nuclear repository purposes. *J Hazard Mater* 2025;**489**:137526.
521 <https://doi.org/10.1016/J.JHAZMAT.2025.137526>
- 522 16. Sidhu HS et al. Minimal changes in microbial abundances and diversity over 7
523 years of emplacement for modules of compacted bentonite exposed to natural
524 groundwater. *Appl Environ Microbiol* 2025;**91**.
525 <https://doi.org/10.1128/AEM.01950-24>
- 526 17. Jalique DR et al. Culturability and diversity of microorganisms recovered from
527 an eight-year old highly-compacted, saturated MX-80 Wyoming bentonite plug.
528 *Appl Clay Sci* 2016;**126**:245–250. <https://doi.org/10.1016/J.CLAY.2016.03.022>
- 529 18. Smart NR et al. The anaerobic corrosion of carbon steel in compacted
530 bentonite exposed to natural Opalinus Clay porewater containing native
531 microbial populations. *Corrosion Engineering Science and Technology*
532 2017;**52**:101–112. <https://doi.org/10.1080/1478422X.2017.1315233>
- 533 19. Frutschi M et al. Microbiological Analysis of Samples from the IC-A Experiment
534 (Iron corrosion in bentonite) at the Mont Terri Rock Laboratory - Final Report.
535 2016.

- 536 20. Burzan N et al. IC-A Experiment - in situ Iron Corrosion in Bentonite, Mont
537 Terri Underground Research Laboratory: Microbial Analysis of Phase 2. 2018.
- 538 21. Reasoner DJ, Geldreich EE. A New Medium for the Enumeration and
539 Subculture of Bacteria from Potable Water. *APPLIED AND ENVIRONMENTAL*
540 *MICROBIOLOGY*. 1985.
- 541 22. Stroes-Gascoyne S et al. The effects of the physical properties of highly
542 compacted smectitic clay (bentonite) on the culturability of indigenous
543 microorganisms. *Appl Clay Sci* 2010;**47**:155–162.
544 <https://doi.org/10.1016/j.clay.2008.06.010>
- 545 23. Medium 63: *Desulfovibrio* (Postgate) medium. 2022. DSMZ, 2022.
- 546 24. Engel K et al. Validating DNA Extraction Protocols for Bentonite Clay.
547 *mSphere* 2019;**4**. <https://doi.org/10.1128/msphere.00334-19>
- 548 25. Babraham Bioinformatics. FastQC - A Quality Control tool for High Throughput
549 Sequence Data. <https://www.bioinformatics.babraham.ac.uk/projects/fastqc/>.
- 550 26. R Core Team. R: A language and environment for statistical computing. 2021.
551 Vienna, Austria.: R Foundation for Statistical Computing. 2021.
- 552 27. Callahan BJ et al. DADA2: High-resolution sample inference from Illumina
553 amplicon data. *Nat Methods* 2016;**13**:581–583.
554 <https://doi.org/10.1038/NMETH.3869>;TECHMETA
- 555 28. Yilmaz P et al. The SILVA and “All-species Living Tree Project (LTP)”
556 taxonomic frameworks. *Nucleic Acids Res* 2014;**42**:D643–D648.
557 <https://doi.org/10.1093/NAR/GKT1209>
- 558 29. Wang Q et al. Naïve Bayesian classifier for rapid assignment of rRNA
559 sequences into the new bacterial taxonomy. *Appl Environ Microbiol*
560 2007;**73**:5261–5267. <https://doi.org/10.1128/AEM.00062-07>
- 561 30. Oksanen J et al. Package ‘vegan’. Community Ecology Package. 2025. 2025.
- 562 31. Pascoal F et al. Definition of the microbial rare biosphere through
563 unsupervised machine learning. *Communications Biology* 2025 **8**:1
564 2025;**8**:544-. <https://doi.org/10.1038/s42003-025-07912-4>
- 565 32. Douglas GM et al. PICRUSt2 for prediction of metagenome functions. *Nature*
566 *Biotechnology* 2020 **38**:6 2020;**38**:685–688. <https://doi.org/10.1038/s41587-020-0548-6>
- 567
- 568 33. Wickham H et al. Welcome to the Tidyverse. *J Open Source Softw*
569 2019;**4**:1686. <https://doi.org/10.21105/JOSS.01686>
- 570 34. Wickham, H. (2016) ggplot2 Elegant Graphics for Data Analysis. Springer-
571 Verlag, New York. - References - Scientific Research Publishing.
572 <https://www.scirp.org/reference/referencespapers?referenceid=3610100>. .
- 573 35. Jakus N et al. Impact of Oxygen Release from Bentonite on Microbial Activity,
574 Mineralogy, and Steel Corrosion. *Environ Sci Technol* 2025;**59**.
575 <https://doi.org/10.1021/ACS.EST.5C08788>
- 576 36. Averhoff B et al. Natural transformation in Gram-negative bacteria thriving in
577 extreme environments: from genes and genomes to proteins, structures and
578 regulation. *Extremophiles* 2021 **25**:5 2021;**25**:425–436.
579 <https://doi.org/10.1007/S00792-021-01242-Z>
- 580 37. Alsharif W, Saad MM, Hirt H. Desert Microbes for Boosting Sustainable
581 Agriculture in Extreme Environments. *Front Microbiol* 2020;**11**:496411.
582 <https://doi.org/10.3389/FMICB.2020.01666>

- 583 38. Bhairamkar S et al. Comprehensive updates on the biological features and
584 metabolic potential of the versatile extremophilic actinomycete *Nocardiopsis*
585 *dassonvillei*. *Res Microbiol* 2024;**175**:104171.
586 <https://doi.org/10.1016/J.RESMIC.2023.104171>
- 587 39. Meklat A et al. *Saccharopolyspora ghardaiensis* sp. nov., an extremely
588 halophilic actinomycete isolated from Algerian Saharan soil. *The Journal of*
589 *Antibiotics* 2014 67:4 2013;**67**:299–303. <https://doi.org/10.1038/ja.2013.136>
- 590 40. Ostrowski M et al. Specific Growth Rate Plays a Critical Role in Hydrogen
591 Peroxide Resistance of the Marine Oligotrophic Ultramicrobacterium
592 *Sphingomonas alaskensis* Strain RB2256. *Appl Environ Microbiol*
593 2001;**67**:1292–1299. <https://doi.org/10.1128/AEM.67.3.1292-1299.2001>
- 594 41. Bush MJ et al. Hyphal compartmentalization and sporulation in *Streptomyces*
595 require the conserved cell division protein SepX. *Nature Communications* 2022
596 13:1 2022;**13**:71-. <https://doi.org/10.1038/s41467-021-27638-1>
- 597 42. Wang X et al. sRNA molecules participate in hyperosmotic stress response
598 regulation in *Sphingomonas melonis* TY. *Appl Environ Microbiol* 2024;**90**.
599 <https://doi.org/10.1128/AEM.02158-23/>
- 600 43. POSTGATE JR. Versatile medium for the enumeration of sulfate-reducing
601 bacteria. *Appl Microbiol* 1963;**11**:265–267.
602 <https://doi.org/10.1128/AM.11.3.265-267.1963>
- 603 44. Wersin P, Mazurek M, Gimmi T. Porewater chemistry of Opalinus Clay
604 revisited: Findings from 25 years of data collection at the Mont Terri Rock
605 Laboratory. *Applied Geochemistry* 2022;**138**.
606 <https://doi.org/10.1016/j.apgeochem.2022.105234>
- 607 45. Mäder UK et al. Interaction of hyperalkaline fluid with fractured rock: Field and
608 laboratory experiments of the HPF project (Grimsel Test Site, Switzerland). *J*
609 *Geochem Explor* 2006;**90**:68–94. <https://doi.org/10.1016/j.gexplo.2005.09.006>
- 610

Supplementary information

Microbial growth inhibition by compacted bentonite after an 8.5-year of *in-situ* incubation

Natalia Jakus^{1*}, Nikitas Diomidis², Rizlan Bernier-Latmani¹

¹Environmental Microbiology Laboratory, École Polytechnique Fédérale de Lausanne (EPFL), Switzerland

²National Cooperative for the Disposal of Radioactive Waste (NAGRA), Switzerland

*Corresponding author: natalia.jakus@epfl.ch

Supplementary Methods

Alpha diversity. Shannon diversity, Simpson diversity, and observed richness (ASV richness) metrics were calculated in R (version 4.5.2) [1] using *vegan* from the filtered ASV count table. Shannon diversity, Simpson diversity, and observed richness (ASV count) were computed per sample. Metadata were matched by sample ID, with starting material treated as a separate density category (Years = 0). Data processing was performed using *readr*, *dplyr*, *tidyr*, and *tibble*, and visualizations were generated in *ggplot2*, with means \pm standard error and individual data points shown.

Supplementary Results and Discussion

Bentonite water content and density

The average observed dry density of the bentonite varied from the theoretical dry density for all modules and yielded $1.34 \pm 0.16 \text{ g/cm}^3$ ($n=3$) for M7 (theoretical value 1.25 g/cm^3), $1.63 \pm 0.16 \text{ g/cm}^3$ ($n=3$) for M8 (1.55 g/cm^3) and a lower value for than expected for M9 (1.45 g/cm^3): 1.40 ± 0.01 ($n=3$). It is important to note that density directly impacts microbial activity, which is why the obtained data were compared with values measured in previous retrieval phases to ensure comparability of microbial data between the phases. The data collected during phase 1 (1.5 years) did not follow the expected values, whereas those from phase 2 (5.5 years) and phase 3 (8.5 years) were closer to the expected value. The most discrepancy was observed for the 1.45 g/cm^3 samples, which is most likely related to the different formulations of the materials: pellets in phase 2 (marked with 'p' for pellets on **Figure S1**) and blocks in phase 3. Note that the method for observed dry density measurements has been improved between phase 1 and phase 2, which may explain the lack of consistency in the data from phase 1. Water content for the deployed bentonite differed depending on the density, with the highest water contents in blocks of lower density. Specific values on the observed dry density and water content collected from bentonite after 8.5 years are in the table (**Table S1**).

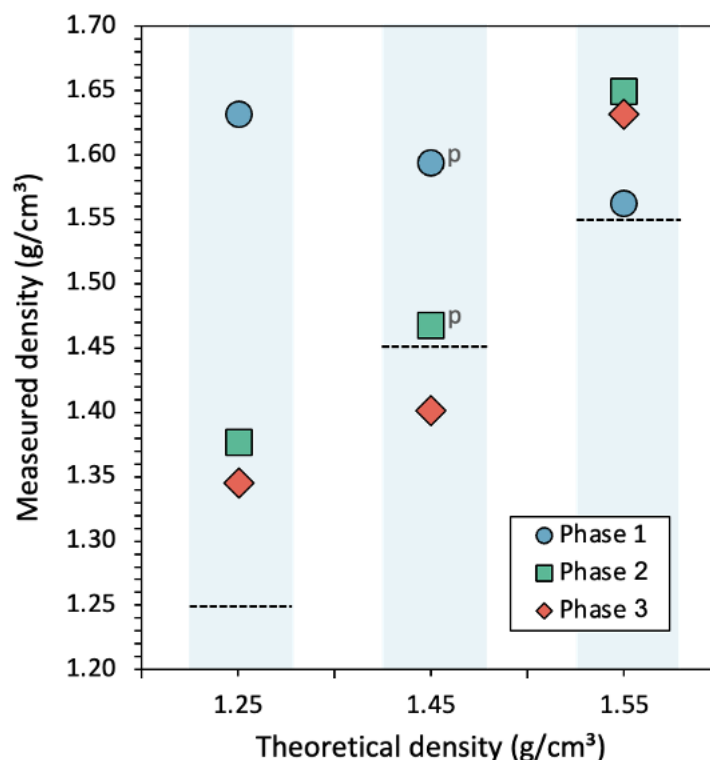


Figure S1. Comparison of observed dry densities measured after the retrieval of modules at three different targeted densities (1.25 , 1.45 and 1.55 g/cm^3) density across three phases (1 (blue circles), 2 (green squares), 3 (orange diamonds)) corresponding to *in-situ* incubation time of 1.5, 5.5 and 8.5 years, respectively. The letter 'p' next to the marker points indicates bentonite in the form of pellets. For all other modules, bentonite in blocks was used. Targeted dry density is indicated by a horizontal dashed line.

Archaeal abundance (qPCR), identity and abundance after 8.5 years of incubation

Archaea 16S rRNA gene copy numbers were, on average, 4- to 3-orders of magnitude lower than bacterial copy numbers, showing that these microorganisms account for only a fraction of the microbial population. Unlike bacteria, the average number of gene copies was not related to density; there was no statistical difference between the different modules nor the external and internal parts of bentonite at any of the tested densities (post-hoc pairwise t-student, $p=0.05$). On average (bulk bentonite, both outer and inner layer combined), the highest numbers were found in pelletized bentonite (1.45 g/cm^3 ; $2.05 \times 10^1 \pm 1.87 \times 10^1$) and the lowest in highly compacted bentonite (1.55 g/cm^3 ; $7.31 \pm 1.17 \times 10^1$). Archaea were identified in bentonite samples (and not porewater) but did not exceed 0.3% of relative abundance except for samples collected from the interior of module M8 (1.55 g/cm^3 , blocks), where they reached 3.8% of relative abundance in the overall microbial community. Interestingly, all detected Archaea are linked to methane or ammonium metabolism. All archaea identified as members of the family of *Methanobacteriaceae*, known to have the genetic potential for formate and hydrogen/carbon dioxide utilization for methanogenesis [2, 3] were related to *Methanobacterium beijingense*, *M. marisnigri* and two unidentified species. Next, *Nitrosopumilaceae* were identified with close relatives to *Candidatus Nitrosotenuis* and other unidentified species, all potential ammonia-oxidizing archaea [4, 5]. Besides that, members of Order *Woesearchaeales* were found, which has been previously proposed to be anaerobic heterotrophs in a potential syntrophic relationship with methanogenic archaea [6].

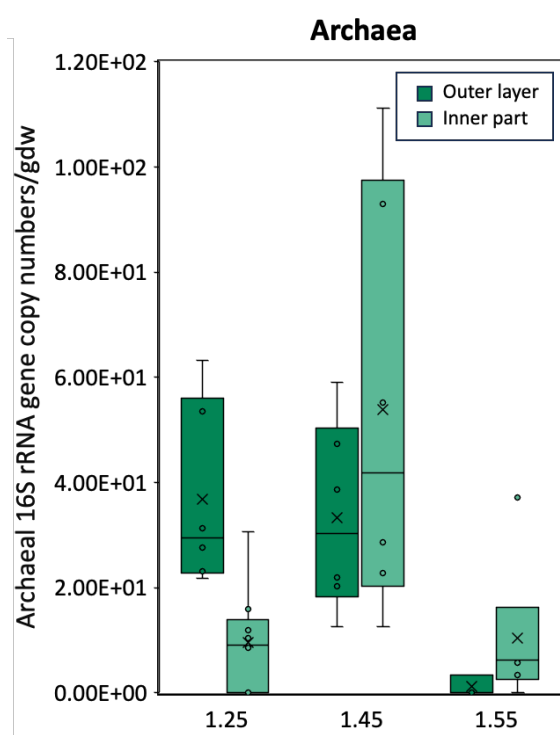


Figure S2. Archaeal abundance as 16S rRNA gene copy numbers per gram of bentonite (dry weight) at varying densities: 1.25 g/cm^3 , 1.45 g/cm^3 and 1.55 g/cm^3 . Data are presented in a box and whisker plot in which the median is indicated with a cross, the mean with a line, each data point with a dot, the box shows the 25th to 75th percentile and the whiskers show the maximum and minimum values of the data.

Microbial community identity and dynamics in compacted bentonite after 5.5 and 8.5 years of incubation

To evaluate absolute changes in the abundance of the top 15 taxa across all bentonite densities and complement the relative abundance analyses presented in the main text, the 16S rRNA gene copy–standardized abundances were compared between the two last time points (**Figure S4**). Consistent with the overall decline in total 16S gene copy numbers, nearly all dominant taxa showed decreased absolute abundances after 8.5 years of incubation compared to 5.5 years, regardless of density. The only exception was *Streptomyces albulus*, whose absolute abundance increased to 2.26×10^4 copies, but only at a density of 1.25 g/cm^3 , making it the most abundant taxon at the 8.5 time point across all densities.

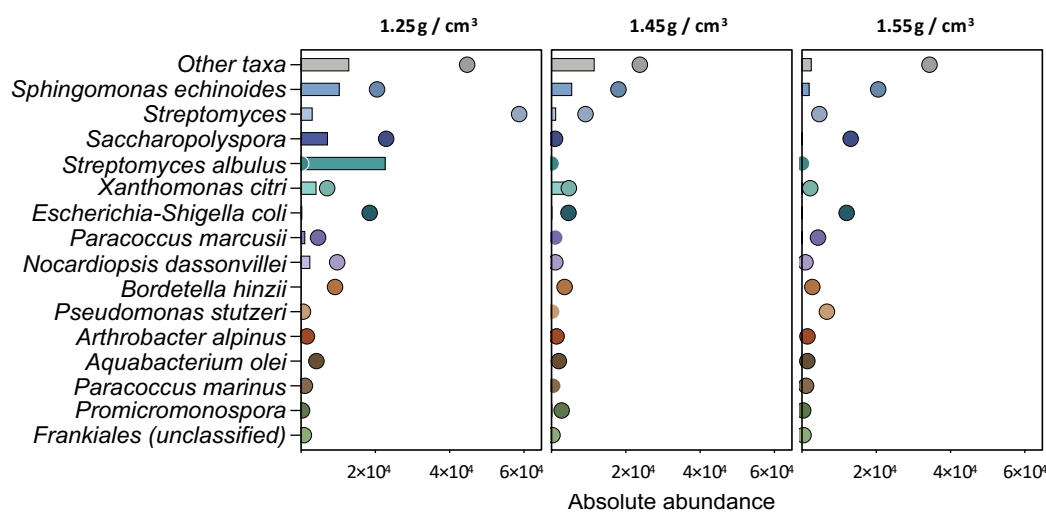


Figure S3. Absolute abundance of the 15 most abundant bacterial taxa across bentonite densities (1.25 , 1.45 , and 1.55 g/cm^3) and porewater; dots indicate 5.5-year samples and bars indicate 8.5-year samples.

Diversity indices after 5.5 and 8.5 years of incubation

At a density of 1.25 g/cm^3 , richness increased over time, whereas both Shannon and Simpson diversity indices decreased. This indicates that although additional taxa became detectable by sequencing, they were predominantly very low in relative abundance, consistent with their classification as members of the rare biosphere. The decline in Shannon and Simpson diversity indices indicates increasing dominance by a small number of taxa, most likely *Streptomyces albulus* and *Sphingomonas echinoides* (**Figure 2C**). Together, these results suggest the progressive specialization of the community, with slow growth of a subset of bacteria (well-adapted to surviving and staying abundant, and very specialized). Note that there are only a few datapoints drawing the average upwards (richness) and downwards (Shannon and Simpson). Without these outliers, the community structure seems to be stable.

At a density of 1.45 g/cm^3 , richness increased or remained high over time, while Shannon diversity stayed high or slightly increased and Simpson diversity showed only a modest decrease. This indicates that although community composition may have changed, overall diversity and evenness were largely maintained. The 1.45 g/cm^3

compaction therefore appears to represent an intermediate regime that is not permissive enough to allow some of the fast-growing taxa to dominate, as observed at lower density, but also not sufficiently restrictive to eliminate most taxa, as observed at higher density.

At 1.55 g/cm³ density, the bentonite community decreased across all indices: richness, Shannon diversity, and Simpson diversity, indicating progressive community decline with a few persistent survivors.

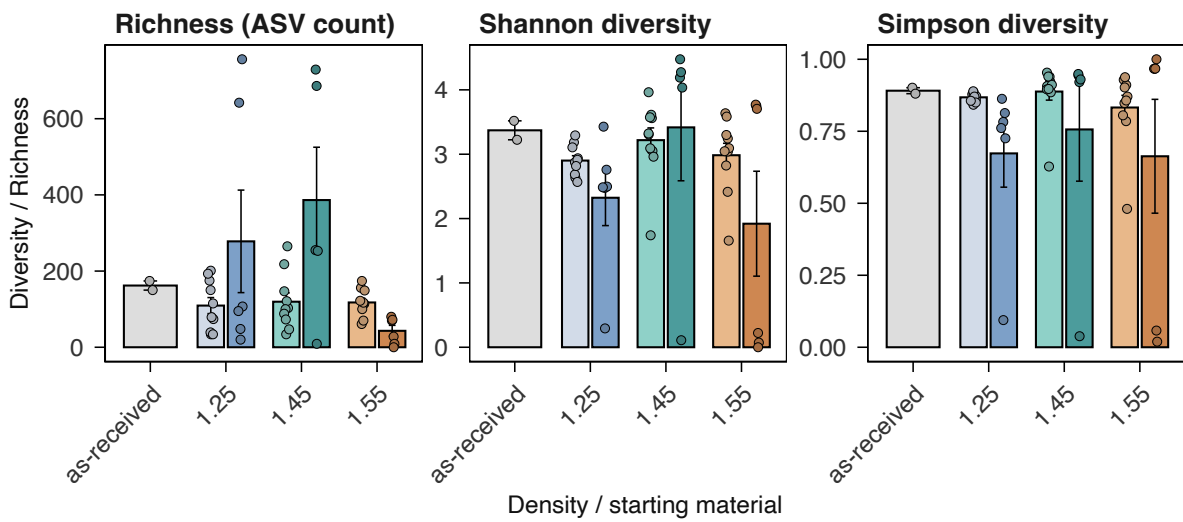


Figure S4. Richness, Shannon, and Simpson diversity indices compared between 5.5 and 8.5 years of *in-situ* incubation.

Supplementary Tables

Table S1. Bulk bentonite dry density was observed after the retrieval of modules together with water content relative to the wet mass and dry bentonite mass. All values are represented by average (n=3), while the errors indicate standard deviation (n=3).

	Theoretical dry density (g/cm ³)	Observed dry density (g/cm ³)	Water content (% _{WT}) *	Water content (% _{DW}) **
M7	1.25 (block)	1.34 ± 0.16	28.22 ± 0.22	39.92 ± 0.43
M8	1.55 (block)	1.63 ± 0.16	18.52 ± 0.04	22.73 ± 0.07
M9	1.45 (pellet)	1.40 ± 0.01	24.87 ± 0.26	33.11 ± 0.46

*Calculated as (weight of water x 100) divided by the weight of the original sample

**Calculated as (weight of water x 100) divided by the weight of the oven-dried (105°C; 24h) sample

Table S2. Significance values (alpha = 0.05) for comparison of cultivation results after 1.5, 5.5 and 8.5 years of the IC-A experiment, using pairwise t-test. The second column shows the compared modules with their specific module ID (e.g., M2, M5, M7) together with years of incubation in parentheses. Modules M7-8 correspond to 8.5 years. Detailed data from earlier time points, together with a detailed description of modules M2-6, can be found in [7].

		Anaerobes		Aerobes		SRB	
		Inner	Outer	Inner	Outer	Inner	Outer
1.25 g/cm ³	M2 (1.5), M5 (5.5)	0.13391185	0.42504814	0.01022871	6.27535E-06	0.73932239	0.20948083
	M5 (5.5), M7 (8.5)	0.18118355	0.42504814	0.00831548	0.003235285	0.04555373	0.03452697
	M2 (1.5), M7 (8.5)	0.00112907	0.05078041	0.29756575	0.0322084	0.05917991	0.06075886
1.55 g/cm ³	M3 (1.5), M6 (5.5)	0.88377157	0.04474357	0.34473069	0.198049924	0.12304841	0.45689076
	M6 (5.5), M8 (8.5)	0.00872301	0.01292808	0.03470127	0.165240569	1.2815E-05	0.01962877
	M3 (1.5), M8 (8.5)	0.00870298	0.11288825	0.8975601	0.26595023	0.07498819	0.05475674

Table S3. Significance values for qPCR comparisons between modules collected across different phases of the IC-A experiment. Materials include reference bentonite (as-received, Years = 0, or 1.5 years where no as-received control was available) and compacted bentonite after 5.5 and 8.5 years of in situ incubation. Modules are abbreviated as M followed by the module ID, with incubation time indicated in brackets. Detailed data from earlier time points used in these analyses are reported in [7].

	Materials compared	Pairwise t-test
Comparison to reference material (as-received)	Reference 1.25 g/cm ³ (0), M7 (8.5)	0.0002378
	Reference 1.45 g/cm ³ (0), M9 (8.5)	0.00948604
	M14 (1.5), M8 (8.5)	0.00047849
Comparison to the last sampling point (5.5 years)	M5 (5.5), M7 (8.5)	0.0002378
	M15 (5.5), M9 (8.5)	0.00948604
	M6 (5.5), M8 (8.5)	0.00047849

Supplementary References

1. R Core Team. R: A language and environment for statistical computing. . 2021. Vienna, Austria.: R Foundation for Statistical Computing, , 2021.
2. Ma K, Liu X, Dong X. Methanobacterium beijingense sp. nov., a novel methanogen isolated from anaerobic digesters. *Int J Syst Evol Microbiol* 2005;55:325–329. <https://doi.org/10.1099/IJS.0.63254-0>
3. Mohammadzadeh R et al. Archaeal key-residents within the human microbiome: characteristics, interactions and involvement in health and disease. *Curr Opin Microbiol* 2022;67:102146. <https://doi.org/10.1016/J.MIB.2022.102146>
4. Sauder LA et al. ‘Candidatus Nitrosotenuis aquarius,’ an Ammonia-Oxidizing Archaeon from a Freshwater Aquarium Biofilter. *Appl Environ Microbiol* 2018;84. <https://doi.org/10.1128/AEM.01430-18>
5. Qin W et al. Candidatus Nitrosopumilaceae. *Bergey’s Manual of Systematics of Archaea and Bacteria* 2016;1–2. <https://doi.org/10.1002/9781118960608.FBM00262>
6. Liu X et al. Insights into the ecology, evolution, and metabolism of the widespread Woese archaeotal lineages. *Microbiome* 2018;6:1–16. <https://doi.org/10.1186/S40168-018-0488-2/FIGURES/6>
7. Burzan N et al. Growth and Persistence of an Aerobic Microbial Community in Wyoming Bentonite MX-80 Despite Anoxic in situ Conditions. *Front Microbiol* 2022;13:1–12. <https://doi.org/10.3389/fmicb.2022.858324>